Qualitative Potential Energy Surfaces. 2. Cycloadditions

N. D. Epiotis* and S. Shaik

Contribution from the Department of Chemistry, University of Washington, Seattle, Washington 98195. *Received January 13, 1977*

Abstract: The linear combination of fragment configurations (LCFC) method is used to construct potential energy surfaces for $[_2\pi_2 + _2\pi_s]$ and $[_2\pi_s + _2\pi_a]$ cycloadditions which constitute models for Huckel antiaromatic and Mobius aromatic thermal reactions as well as models of Hückel aromatic and Mobius antiaromatic photochemical reactions. The factors which control the heights of barriers and the stabilities of possible intermediates in thermal reactions are discussed. More importantly, an understanding of the key features of photochemical reactions is now made possible. In this connection, it is shown that barrier heights as well as decay efficiencies play crucial roles.

I. Introduction

Cycloadditions constitute the class of chemical reactions which poses the most formidable challenge to the mechanistic and theoretical chemist. This is due to the fact that the union of two cycloaddends can occur in any one of many different stereochemical and regiochemical ways. Hence, the rationalizations or predictions of the preferred product of a given cycloaddition reaction might appear to be an impossible task. Nevertheless, significant progress has been made in this area since the publication of the Woodward–Hoffmann rules in 1965.[1] However, despite these recent developments, certain features of thermal cycloadditions and even more aspects of photocycloadditions have refused to yield to a single, all-encompassing interpretation.

In this work, we use the linear combination of fragment configurations (LCFC) method discussed in a previous paper[2] for constructing the PE surfaces of the model $[_2\pi_s + _2\pi_s]$ and $[_2\pi_s + _2\pi_a]$ cycloadditions. A discussion of possible mechanisms of thermal and photochemical aromatic and antiaromatic reactions is presented.

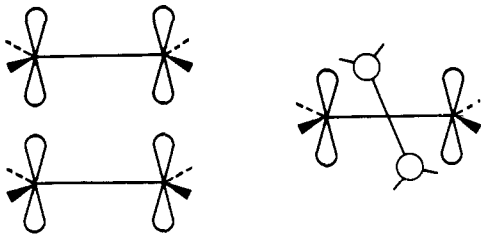

$[_2\pi_s + _2\pi_s]$ $\qquad$ $[_2\pi_s + _2\pi_a]$

II. Theory

For illustrative purposes, we use the singlet cyclodimerization reaction of ethylene as the model reaction assuming that the two molecules approach each other in a symmetric fashion.

The first task is the specification of the basis set of singlet zero-order configurations to be employed in the analysis. These are shown in Figure 1. The final symmetry and spin-adapted configurations[3] are given below:

$$\Psi_1 = D_1D_2$$

$$\Psi_2^+ = \frac{1}{(2)^{1/2}}(D_1^+D_2^- + D_1^-D_2^+)$$

$$\Psi_2^- = \frac{1}{(2)^{1/2}}(D_1^+D_2^- - D_1^-D_2^+)$$

$$\Psi_3^+ = \frac{1}{(2)^{1/2}}(D_1^*D_2 + D_1D_2^*)$$

$$\Psi_3^- = \frac{1}{(2)^{1/2}}(D_1^*D_2 - D_1D_2^*)$$

$$\Psi_4^+ = \frac{1}{(2)^{1/2}}(D_1^{+2}D_2^{-2} + D_1^{-2}D_2^{+2})$$

$$\Psi_4^- = \frac{1}{(2)^{1/2}}(D_1^{+2}D_2^{-2} - D_1^{-2}D_2^{+2})$$

$$\Psi_5^+ = \frac{1}{(2)^{1/2}}(D_1^{**}D_2 + D_1D_2^{**})$$

$$\Psi_5^- = \frac{1}{(2)^{1/2}}(D_1^{**}D_2 - D_1D_2^{**})$$

$$\Psi_6^+ = \frac{1}{(2)^{1/2}}(D_1^{+*}D_2^- + D_1^-D_2^{+*})$$

$$\Psi_6^- = \frac{1}{(2)^{1/2}}(D_1^{+*}D_2^- - D_1^-D_2^{+*})$$

$$\Psi_7^+ = \frac{1}{(2)^{1/2}}(D_1^+D_2^{-*} + D_1^{-*}D_2^+)$$

$$\Psi_7^- = \frac{1}{(2)^{1/2}}(D_1^+D_2^{-*} - D_1^{-*}D_2^+)$$

$$\Psi_8 = D_1^*D_2^*$$

For simplicity, we include only the lower energy "ditriplet" $D_1^*D_2^*$ surface and neglect the higher "disinglet" one.

The various zero-order configurations fall within three sets. One set includes only the no-bond configuration, D_1D_2. The second set includes configurations which arise by promoting one electron to a higher energy MO. Henceforth, such configurations will be termed collectively monoexcited configurations. The third set includes configurations which arise by promoting two electrons to higher energy MOs. Henceforth, such configurations will be termed collectively diexcited configurations. These three sets will be taken to define three packets, Λ_1, Λ_2, and Λ_3.

The shape of the various types of diabatic surfaces has been discussed in the previous paper.[2] It was concluded that no-bond (e.g., D_1D_2) and locally excited (e.g., $\Psi_3^\pm$ and $\Psi_5^\pm$) type diabatic curves are repulsive. On the other hand, the charge transfer (e.g., $\Psi_2^\pm$ and $\Psi_6^\pm$) type diabatic curves display a minimum. The shape of the final adiabatic PE surfaces depends on the interactions between the diabatic surfaces and this, in turn, is characteristic of the stereochemical path. The interaction matrix is shown in Table I[4] and the intra- and in-

0002-7863/78/1500-0009$01.00/0

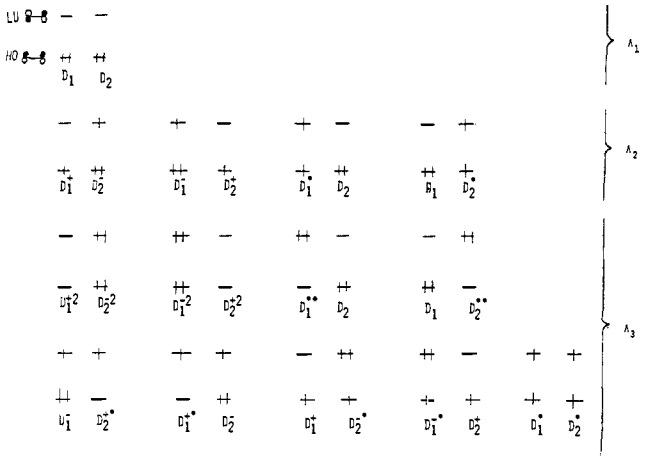

Figure 1. Zero-order configurations for the $[2\pi + 2\pi]$ dimerization of ethylene. Λ_1, Λ_2, and Λ_3 are configuration packets.

Chart I

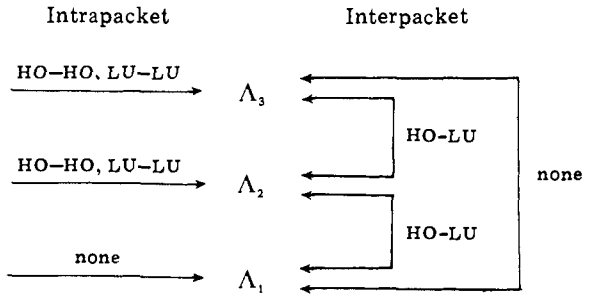

$$\text{HO-HO} \begin{cases} \neq 0[_2\pi_s + {}_2\pi_s] \\ \text{LU-LU} \quad = 0[_2\pi_s + {}_2\pi_a] \end{cases}$$

$$\text{HO-LU} \begin{cases} = 0[_2\pi_s + {}_2\pi_s] \\ \neq 0[_2\pi_s + {}_2\pi_a] \end{cases}$$

terpacket interactions are schematically depicted in Chart I.

II.1. Construction of Adiabatic PE Surfaces. We first consider the $[_2\pi_s + {}_2\pi_s]$ geometry of approach and intrapacket interactions. The Λ_1 packet contains only Ψ_1, so there are no intrapacket interactions. The Λ_2 packet contains four configurations which can interact strongly in a HO–HO and LU–LU sense. Similarly, the Λ_3 packet contains nine configurations which can interact also in a HO–HO and LU–LU sense. On the other hand, the interactions between the diabatic surfaces of Λ_1 and Λ_2, as well as those between the diabatic surfaces of Λ_2 and Λ_3, are of the HO–LU type and, hence, zero. Accordingly, it follows that in the case of the $[_2\pi_s + {}_2\pi_s]$ geometry, the diabatic surfaces within each packet interact strongly whereas those belonging to different packets do not interact. As the two ethylenes approach each other, spatial overlap increases and intrapacket interactions continuously increase, while interpacket interactions remain always zero. As a result, the Λ_2 and Λ_3 packets "swell" and their boundaries travel toward the Ψ_1 diabatic surface. Eventually the boundary of the Λ_3 packet will define the potential well where the product will lie and Λ_2 will define the potential well where an excited intermediate will be accommodated. The resulting PE surfaces which describe the photochemical and thermal $[_2\pi_s + {}_2\pi_s]$ cycloadditions can be represented as shown in Figure 2.

The various features of the PE surfaces can be conveyed by the following chemical equations, where a wavy line signifies radiationless decay.

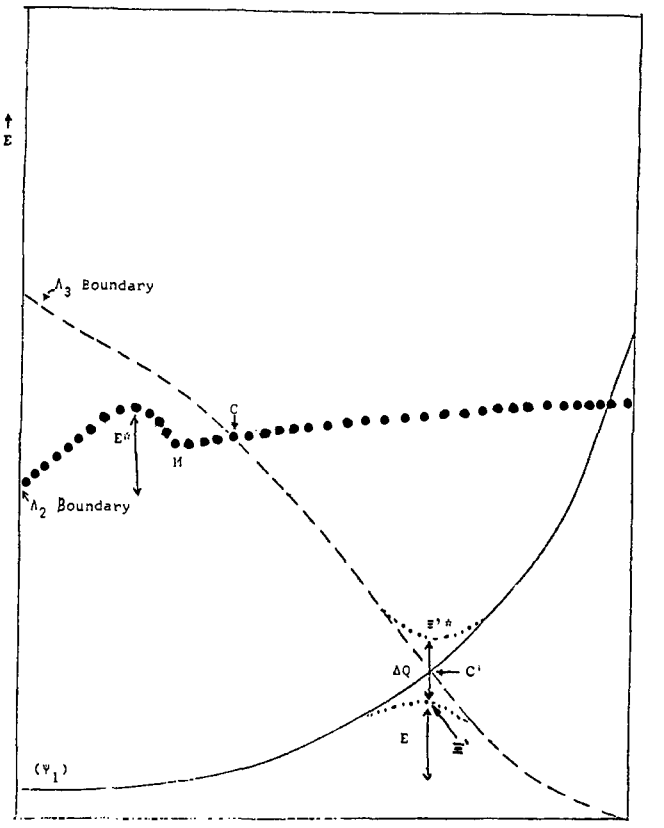

Figure 2. PE surfaces for thermal and photochemical $[_2\pi_s + {}_2\pi_s]$ cyclodimerization of ethylene. The "parent" diabatic surfaces at infinite intermolecular distance are shown in parentheses. C′ is the point of the Ψ_1–Λ_3 boundary avoided crossing (dotted lines). C is the crossing point of the first excited surface with the Λ_3 boundary. Diagram is schematic.

(a) Thermal $[_2\pi_s + {}_2\pi_s]$

$$D_1 + D_2 \rightarrow (D_1 \cdots D_2) \rightarrow C_4H_8$$

(b) Photochemical $[_2\pi_s + {}_2\pi_s]$

$$D_1 + D_2^* \rightarrow (D_1 \cdots D_2^*) \rightarrow M \rightarrow \equiv'^* \longrightarrow [\equiv'] \begin{cases} \rightarrow D_1 + D_2 \\ \rightarrow C_4H_8 \end{cases}$$

$$(D_1 \cdots D_2^*) \rightarrow D_1 + D_2 \qquad M \rightarrow D_1 + D_2$$

In the above equations, $(D_1 \cdots D_2)$ is a thermal encounter complex which can be weakly bound and $(D_1 \cdots D_2^*)$ is an excited encounter complex which also can be weakly bound.[1]

Let us now consider in some detail the features of the ground and lowest excited surfaces of $[_2\pi_s + {}_2\pi_s]$ cycloaddition. The ground surface displays a barrier E which is produced by the pseudocrossing of the Λ_1 and Λ_3 packets. The key feature of the excited surface can be understood by examining the intrapacket interactions of Λ_2. The avoided crossing of the Ψ_2^- and Ψ_3^- diabatic surfaces leads to formation of a barrier, E^*, and an excited intermediate, M.[5] If the interaction of Ψ_2^- and Ψ_3^- is very strong, the barrier will be negligible. Past the minimum describing the excited intermediate, M, the boundary of Λ_2 crosses the boundary of Λ_3 and this is a real crossing. This is the point at which the reaction system makes the transition to the boundary of Λ_3 and is ultimately led to become an excited intermediate $\equiv'^*$.[6] This can now decay to the ground surface and the efficiency of the decay will depend on the energy gap ΔQ,[7,8] the magnitude of which is controlled by the two-electron interaction of the Λ_1 and Λ_3 packets.

Table I. Interaction Matrix for $[2\pi + 2\pi]$ Cyclodimerization of Ethylene

	Ψ_1	Ψ_2^+	Ψ_2^-	Ψ_3^+	Ψ_3^-	Ψ_4^+	Ψ_4^-	Ψ_5^+	Ψ_5^-	Ψ_6^+	Ψ_6^-	Ψ_7^+	Ψ_7^-	Ψ_8
Ψ_1		$(HO^{D_1}\text{-}LU^{D_2}) + (HO^{D_2}\text{-}LU^{D_1})$	0	0	0	0	0	0	0	0	0	0	0	0
Ψ_2^+			0	0	0	$(HO^{D_1}\text{-}LU^{D_2}) + (HO^{D_2}\text{-}LU^{D_1})$	0	0	0	0	0	0	0	$(HO^{D_2}\text{-}LU^{D_1} + (HO^{D_1}\text{-}LU^{D_2}$
Ψ_2^-				0	$(HO^{D_1}\text{-}HO^{D_2}) + (LU^{D_1}\text{-}LU^{D_2})$	0	$(HO^{D_1}\text{-}LU^{D_2}) + (HO^{D_2}\text{-}LU^{D_1})$	0	0	0	0	0	0	0
Ψ_3^+					0	0	0	0	0	$(HO^{D_1}\text{-}LU^{D_2}) + (HO^{D_2}\text{-}LU^{D_1})$	0	0	0	0
Ψ_3^-						0	0	0	0	0	$(HO^{D_1}\text{-}LU^{D_2}) + (HO^{D_2}\text{-}LU^{D_1})$	0	$(HO^{D_1}\text{-}LU^{D_2}) + (HO^{D_2}\text{-}LU^{D_1})$	0
Ψ_4^+							0	0	0	$LU^{D_1}\text{-}LU^{D_2}$	0	$HO^{D_1}\text{-}HO^{D_2}$	0	0
Ψ_4^-								0	0	0	$LU^{D_1}\text{-}LU^{D_2}$	0	$HO^{D_1}\text{-}HO^{D_2}$	0
Ψ_5^+									0	$(LU^{D_1}\text{-}LU^{D_2}) + (HO^{D_1}\text{-}HO^{D_2})$	0	$(LU^{D_1}\text{-}LU^{D_2}) + (HO^{D_1}\text{-}HO^{D_2})$	0	0
Ψ_5^-										$(LU^{D_1}\text{-}LU^{D_2}) + (HO^{D_1}\text{-}HO^{D_2})$	0	$(LU^{D_1}\text{-}LU^{D_2}) + (HO^{D_1}\text{-}HO^{D_2})$	0	0
Ψ_6^+											0	0	0	$(HO^{D_1}\text{-}HO^{D_2} + (LU^{D_1}\text{-}LU^{D_2}$
Ψ_6^-												0	0	0
Ψ_7^+													0	$(HO^{D_1}\text{-}HO^{D_2} + (LU^{D_1}\text{-}LU^{D_2}$
Ψ_7^-														0
Ψ_8														

We next consider the $[_2\pi_s + _2\pi_a]$ geometry of approach. Once again, the Λ_1 packet contains only Ψ_1, so there are no intrapacket interactions. The Λ_2 packet contains four configurations and all the possible one-electron interaction matrix elements are of the HO-HO or LU-LU type, and, hence, zero. The same situation exists in the case of intrapacket interactions in Λ_3. Contrary to the case of $[_2\pi_s + _2\pi_s]$ cycloadditions, the diabatic surfaces within each packet do not interact when the two ethylenes approach each other in a $[_2\pi_s + _2\pi_a]$ manner.

The interpacket interactions also differ from those which obtain in the $[_2\pi_s + _2\pi_s]$ geometry. For example, consider the interaction of Ψ_1 of Λ_1 with Ψ_2^+, Ψ_2^-, Ψ_3^+, and Ψ_3^-, of Λ_2. The possible interaction matrix elements will be large, since the HO-LU overlap integral is large. The same argument applies to the interaction between diabatic surfaces of Λ_2 and those of Λ_3. As the two molecules approach each other, interpacket interactions progressively increase, while intrapacket interactions remain always zero. As a result, the three packets "repel" each other. The PE surfaces for photochemical and thermal $[_2\pi_s + _2\pi_a]$ cycloadditions are shown in Figure 3. The details of the PE surfaces can be expressed as follows:

$$D_1 + D_2 \longrightarrow (D_1 \cdots D_2) \longrightarrow C_4H_8$$

$$D_1 + D_2^* \longrightarrow (D_1 \cdots D_2^*) \longrightarrow O \begin{cases} \nearrow C_4H_8 \\ \searrow D_1 + D_2 \end{cases}$$

$$\Big\downarrow\Big\downarrow$$

$$D_1 + D_2$$

The PE surface aspects of the $[_2\pi_s + _2\pi_a]$ cycloaddition are simple to understand. The barrier of the thermal reactions, E, arises primarily from the interaction of the Ψ_1 and Ψ_2^+ diabatic surfaces. The photochemical barrier, E^*, arises from the crossing of the charge transfer and locally excited diabatic

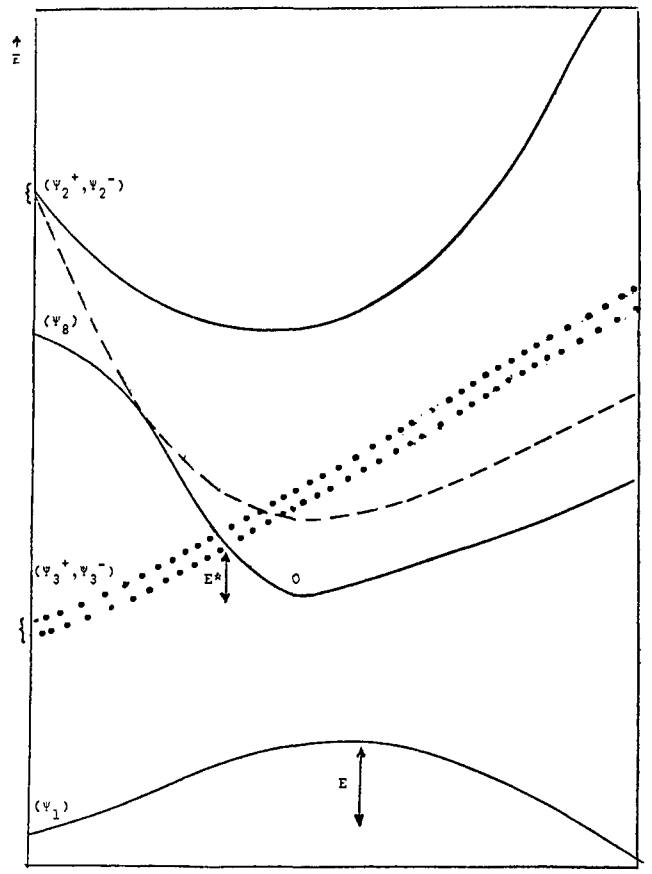

Figure 3. PE surfaces for thermal and photochemical $[_2\pi_s + _2\pi_a]$ dimerization of ethylene. The corresponding diabatic surfaces at infinite intermolecular distance are shown in parentheses. Diagram is schematic.

surfaces, and its height is controlled by the interaction of the Ψ_1, Ψ_2^+, and Ψ_8 diabatic surfaces. Decay of the excited intermediate, O,[9] to the ground adiabatic surface completes the sequences of events.

While we have restricted our attention to the $[_2\pi_s + _2\pi_s]$ and $[_2\pi_s + _2\pi_a]$ mechanism of cyclobutane formation, a third, stepwise mechanism exists. Henceforth, we shall refer to the

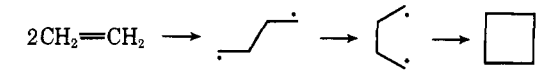

TB

above mechanism as the TB mechanism and the first elementary step as the TB step.

Following familiar arguments, we can show that in bicentric reactions, both intra- and interpacket interactions obtain. Accordingly, the PE surfaces of the thermal and photochemical TB step can be constructed in the same manner as in the case of $[_2\pi_s + _2\pi_a]$ cycloaddition.

Having discussed the PE surfaces for $[_2\pi_s + _2\pi_s]$, TB, and $[_2\pi_s + _2\pi_a]$ cycloaddition, the question arises as to which of the three stereochemical paths is favored. In the case of the thermal reaction, it is clear that only the height of the ground surface barrier has to be considered. While an a priori prediction cannot be made, it is reasonable to assume that interpacket interactions will produce the lowest barrier in the case of $[_2\pi_s + _2\pi_a]$ cycloaddition. The prediction of the relative efficiencies of the $[_2\pi_s + _2\pi_s]$, TB, and $[_2\pi_s + _2\pi_a]$ photoreactions is more straightforward. In this instance, one has to be concerned with two aspects of the reaction, namely, the barrier on the lowest excited surface and the decay to ground surface. The $[_2\pi_s + _2\pi_s]$ stereochemical path is favored on both counts: the heights of the photochemical barriers are optimum and the efficiency of decay is maximum since the reaction system can find a

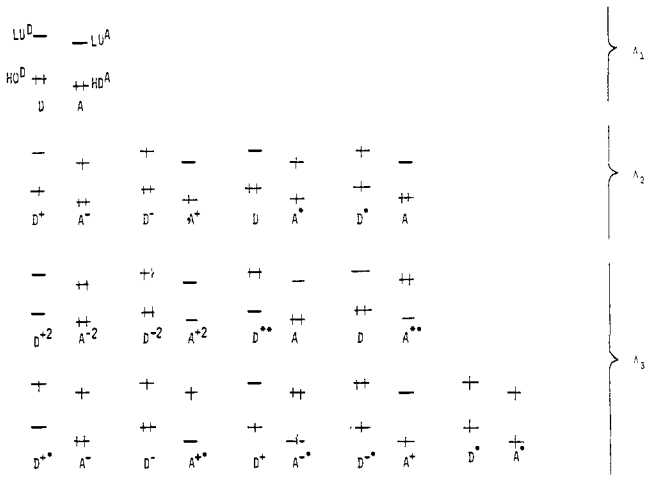

Figure 4. Zero-order configuration for the $[2\pi + 2\pi]$ cycloadditions of a donor olefin (D) and an acceptor olefin (A).

"hole"[8] for efficient decay to the ground surface, i.e., it can arrive at a point (intermediate $\equiv'^*$) where two adiabatic surfaces are separated by a small energy gap, and, hence, decay from the upper to lower surface is expected to be fast.

The above considerations lead naturally to the formation of two rules: (a) The preferred stereochemical pathway of a thermal reaction will be the one which maximizes interpacket interactions. (b) The preferred stereochemical pathway of a photochemical reaction will be the one which maximizes intrapacket interactions and minimizes interpacket interactions. A reaction path which is favorable by reference to the above rules will be termed aromatic. Paths which fulfill the contrary conditions will be termed antiaromatic.

II.2. The Effect of Polarity. Potential Energy Surfaces for Nonionic and Ionic $[2\pi + 2\pi]$ Cycloadditions. We now inquire as to how the conclusions of the previous analysis will be modified when polarity is increased, i.e., when one ethylene is replaced by a donor olefin and the other by an acceptor olefin. The basis set configurations appropriate to this problem are shown in Figure 4. Increasing polarity causes energy depression of D^+A^-, and $D^{+*}A^-$, and $D^{+2}A^{-2}$ type diabatic surfaces and results in energy lowering of the corresponding adiabatic surfaces. Ultimately, D^+A^- will cross DA, marking the transition from a nonionic to an ionic cycloaddition. Similarly, ionic cycloaddition can materialize also when the D^+A^- lies very near the DA diabatic surface and the interaction of the D^+A^- and DA* diabatic surfaces causes the adiabatic surface originating from the D^+A^- diabatic surface to cross the adiabatic surface originating from the DA diabatic surface. The same effect can be reproduced by an increase in solvent polarity.[10] These considerations are illustrated in Figures 5 and 6.

The mechanistic features of ionic cycloaddition reactions can be conveyed by the following chemical equations:

(a) Ionic thermal $[_2\pi_s + _2\pi_s]$ cycloaddition

$$D + A \rightarrow (D \cdots A) \rightarrow M \rightarrow P \qquad (P = \text{product})$$

(b) Ionic photochemical $[_2\pi_s + _2\pi_s]$ cycloaddition

$$D + A^* \longrightarrow (D \cdots A^*) \longrightarrow M \longrightarrow P$$
$$\Downarrow\Downarrow$$
$$D + A$$

(c) Ionic thermal $[_2\pi_s + _2\pi_a]$ cycloaddition[11]

$$D + A \rightarrow (D \cdots A) \rightarrow N^* \rightarrow P$$

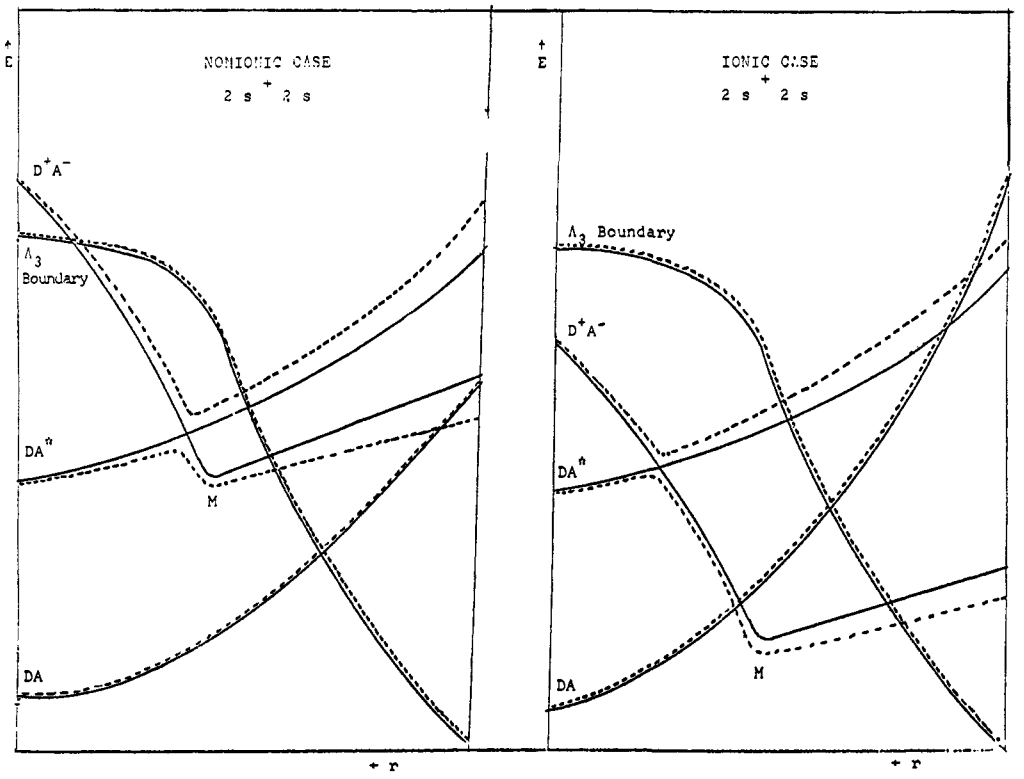

Figure 5. The effect of polarity on the shapes of the PE surfaces for $[_{2}\pi_{s} + _{2}\pi_{s}]$ cycloadditions. Solid lines indicate diabatic and dashed lines adiabatic surfaces. Two-electron interactions are neglected. Diagrams are schematic

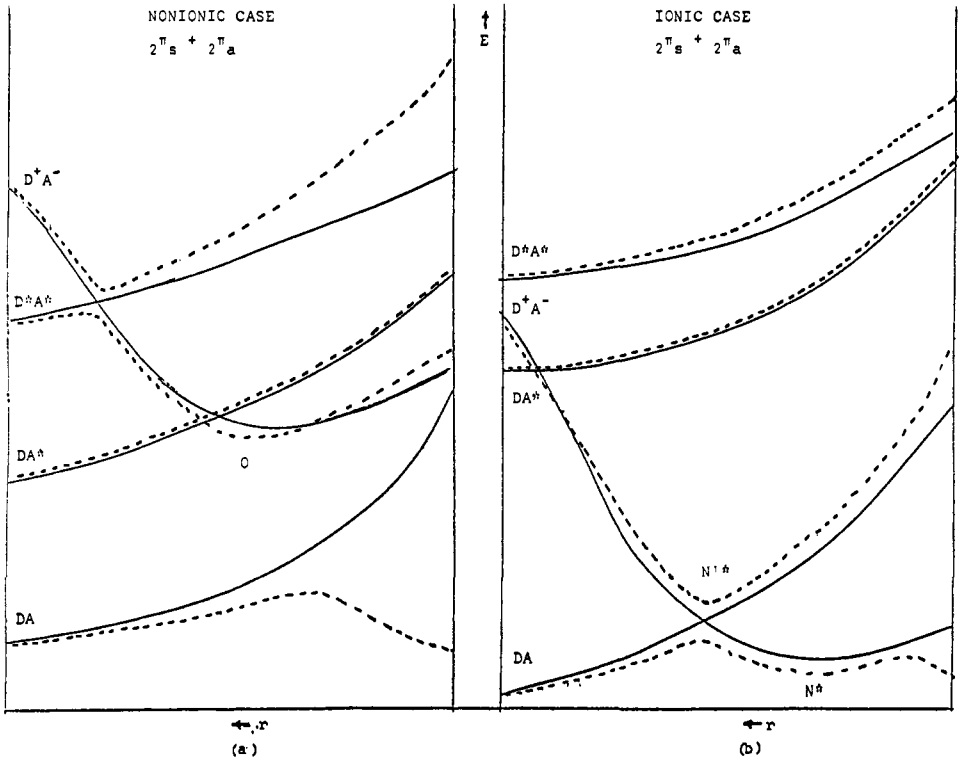

Figure 6. The effect of polarity on the shapes of the potential energy surfaces for $[_{2}\pi_{s} + _{2}\pi_{a}]$ cycloaddition. Solid lines indicate diabatic and dashed lines adiabatic surfaces. Two-electron interactions are neglected. Diagrams are schematic.

(d) Ionic photochemical $[_{2}\pi_{s} + _{2}\pi_{a}]$ cycloaddition[12]

$$\begin{array}{ccccccc} D + A^{*} & \longrightarrow & (D\cdots A^{*}) & \longrightarrow & N'^{*} & \longrightarrow & N^{*} \longrightarrow P \\ & & \downarrow\downarrow & & \downarrow & & \\ & & D + A & & D + A & & \end{array}$$

In dealing with thermal ionic cycloadditions, we must assume that intermediate formation is rate determining. However, situations may arise where intermediate closure is rate determining. Thus, we should define two different types of ionic $[2\pi + 2\pi]$ cycloadditions: (a) type A ionic cycloadditions, where intermediate M or N* formation is rate determining;

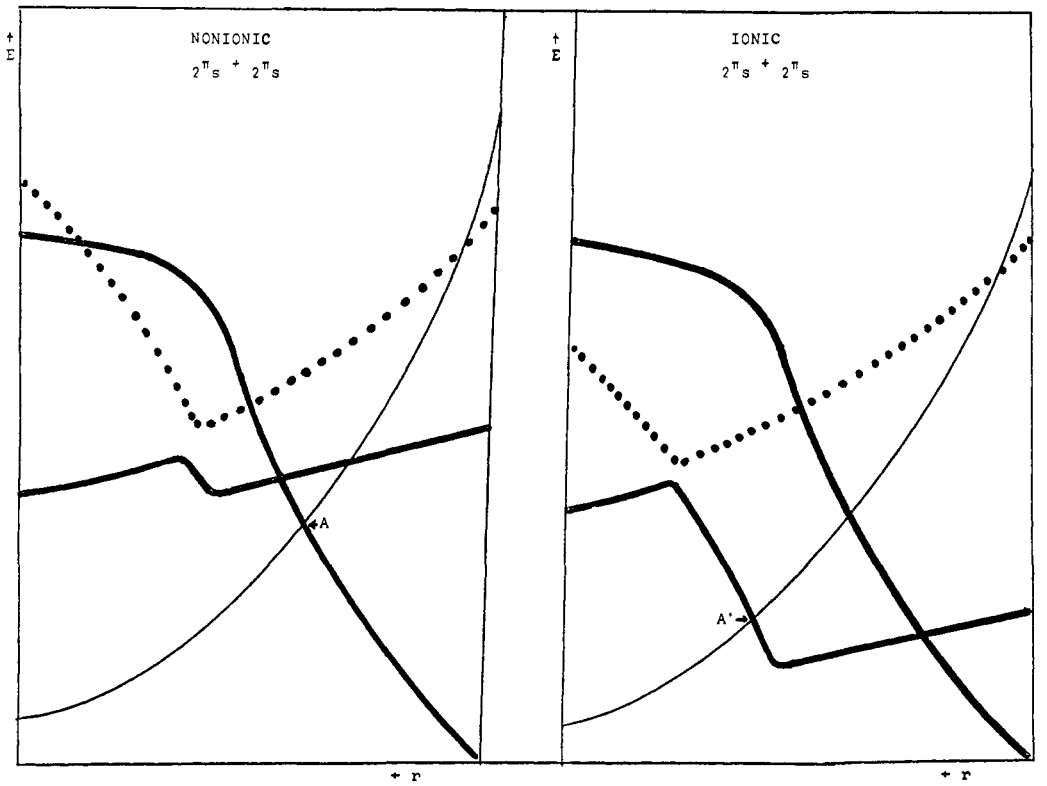

Figure 7. Path pericyclicities in $[_2\pi_s + _2\pi_s]$ cycloaddition. Solid line = nonpericyclic; thick line = pericyclic; dotted line = antipericyclic. Diagrams are schematic

(b) type B ionic cycloadditions, where collapse of the intermediate to product is rate determining. We shall limit the discussion to type A ionic reactions. However, similar arguments can be applied to type B reactions.

II.3. Pericyclic, Effectively Pericyclic and Quasi-Pericyclic Reactions. An important concept which can be formulated with reference to qualitative PE surfaces is the concept of pericyclicity. In Figures 7 and 8 we depict the parts of adiabatic surfaces which involve pericyclic bonding and those which do not. The following trends are noteworthy:

(a) In the case of thermal nonionic $[_2\pi_s + _2\pi_s]$ cycloaddition, the reaction system jumps from a nonpericyclic[13] surface to a pericyclic[13] surface in the neighborhood of A. As polarity increases, this transition occurs earlier in the reaction coordinate, while simultaneously the height of the thermal barrier decreases.

(b) In the case of thermal ionic $[_2\pi_s + _2\pi_s]$ cycloaddition, the reaction system jumps from a nonpericyclic surface to a pericyclic surface in the neighborhood of A', i.e., very early on the reaction coordinate. In this case, the reaction system finds itself on a pericyclic surface since the very early stage of the reaction.

(c) In the case of photochemical nonionic or ionic $[_2\pi_s + _2\pi_s]$ cycloadditions, the reaction complex travels on a surface which is entirely pericyclic.

(d) In the case of thermal nonionic or ionic $[_2\pi_s + _2\pi_a]$ cycloadditions, the reaction complex travels on a surface which is entirely pericyclic.

(e) In the case of photochemical nonionic $[_2\pi_s + _2\pi_a]$ cycloadditions, and assuming a dominant interaction of D^+A^- with D*A*, the reaction system jumps from a nonpericyclic to a pericyclic surface in the neighborhood of B. This transition occurs very early on the reaction coordinate.

(f) In the case of photochemical ionic $[_2\pi_s + _2\pi_a]$ cycloaddition, the reaction system jumps from a nonpericyclic onto a surface which is initially pericyclic and subsequently becomes antipericyclic.

The analysis presented above provides grounds for an important classification of chemical reactions. Thus, we can distinguish the following reaction types:

(a) A pericyclic reaction is the one which proceeds entirely on a pericyclic path, i.e., a path which is defined by a sequence of points each corresponding to a pericyclic electronic state. Thermal, nonionic and ionic, $[_2\pi_s + _2\pi_a]$ cycloadditions are all pericyclic reactions.

(b) An effectively pericyclic reaction is the one which proceeds mostly, but not entirely, on a pericyclic path. In such a reaction, the two reactants approach each other on a nonpericyclic path, i.e., a path defined by a sequence of points each corresponding to a nonpericyclic electronic state. When spatial overlap between the two reactants is still small, the reaction complex makes a transition to a pericyclic path. In general, this transition occurs at the top of a barrier. Thermal ionic $[_2\pi_s + _2\pi_s]$ cycloadditions are examples of effectively pericyclic reactions.

(c) A quasi-pericyclic reaction is the one which proceeds to a large extent on a nonpericyclic path. In such a reaction, the two reactants approach each other on a nonpericyclic path and a transition to a pericyclic path occurs late in the reaction when spatial overlap between the two reactants is very large. This transition occurs at the top of a barrier. Thermal nonionic $[_2\pi_s + _2\pi_s]$ cycloadditions are examples of quasi-pericyclic reactions.

III. Mechanisms of Stereochemical Nonretention in Cycloadditions

The analysis presented above can be condensed in two rules:

(a) *A reaction complex which finds itself on an antipericyclic or nonpericyclic path will tend to distort so that the total energy will decrease. If such a distortion occurs at long intermolecular distances, stereorandomization due to torsional motions within each reactant will be minimal. By contrast, if*

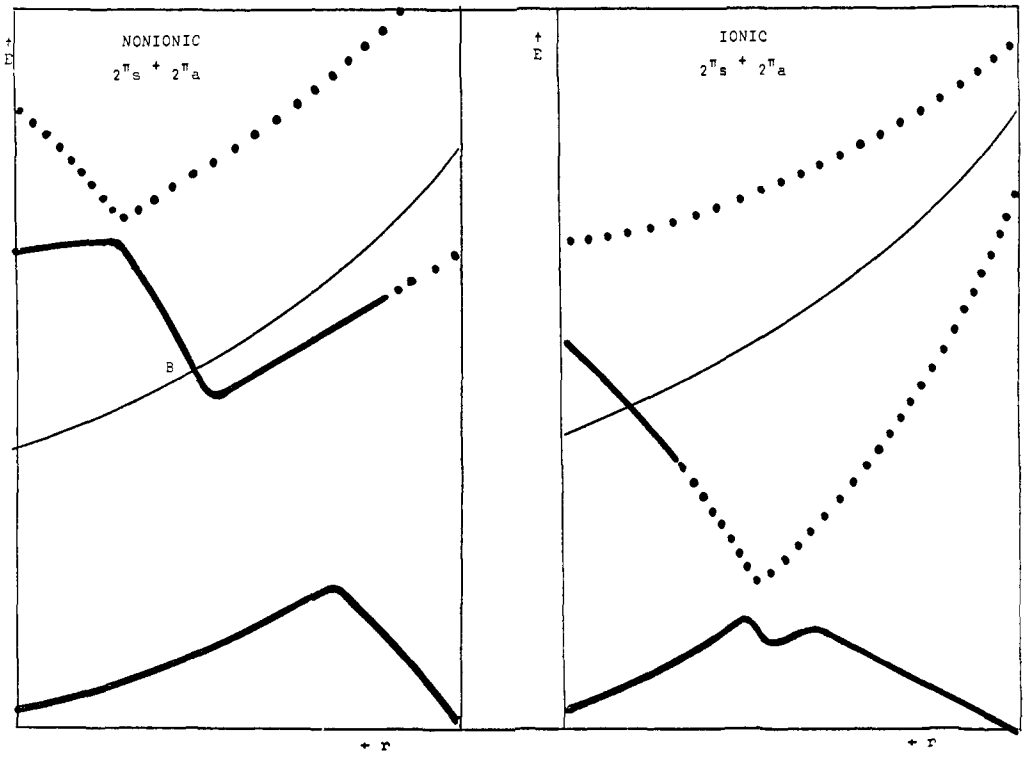

Figure 8. Path pericyclicities in $[_2\pi_s + _2\pi_a]$ cycloaddition. Solid line = nonpericyclic; thick line = pericyclic; dotted line = antipericyclic. Diagrams are schematic

distortion occurs at short intermolecular distances, stereorandomization will be pronounced.

(b) *A reaction complex which finds itself on a pericyclic path will tend not to distort unless the interaction of the diabatic surfaces which produces the pericyclic adiabatic pericyclic surface is weak. In this case, stereorandomization will be zero or small.*

The chemical consequences of these rules can be illustrated by means of a specific example. To this extent, consider a distorted U-like structure in the neighborhood of the transition state of a quasi-pericyclic (U″) and an effectively pericyclic

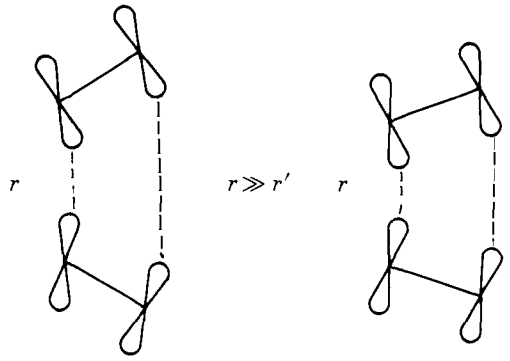

U′ effectively pericyclic reaction U″ quasi-pericyclic reaction

(U′) $[_2\pi_s + _2\pi_s]$ cycloaddition. As can be seen, U′ is looser than U″. Obviously, U′ resembles more two reactant molecules, both having nearly fully formed π bonds, while U″ resembles more a cisoid diradicaloid intermediate having no π bonds. Hence, bond rotation in U″ is expected to be more facile than in U′. Accordingly, stereorandomization is expected to be appreciable in the case of a quasi-pericyclic $[_2\pi_s + _2\pi_s]$ cycloaddition. By contrast, effectively pericyclic reactions may be as stereoselective as true pericyclic reactions.

IV. Discussion

The most important chemical implications of this work are the following:

(a) In a case of a *nonionic* $[_2\pi_s + _2\pi_a]$ approach, either cycloaddend can act as the antarafacial component, unless steric effects select one of the two possible modes. Accordingly, in most cases, competing $[_2\pi_s + _2\pi_a]$ mechanisms may result in loss of reactant stereochemistry in the final product. In the case of a nonionic TB approach, bond rotation can readily occur, and such an approach is expected to be responsible for nonstereoselective reaction. Finally, in the case of a nonionic $[_2\pi_s + _2\pi_s]$ approach, bond rotation may occur giving rise also to nonstereoselective product formation. Clearly, any one of the three mechanisms may give rise to a low degree of stereoretention. In other words, *the stereochemical criterion for distinguishing nonionic* $[2\pi + 2\pi]$ *cycloaddition pathways is inadequate when applied by itself.*

Scheme I

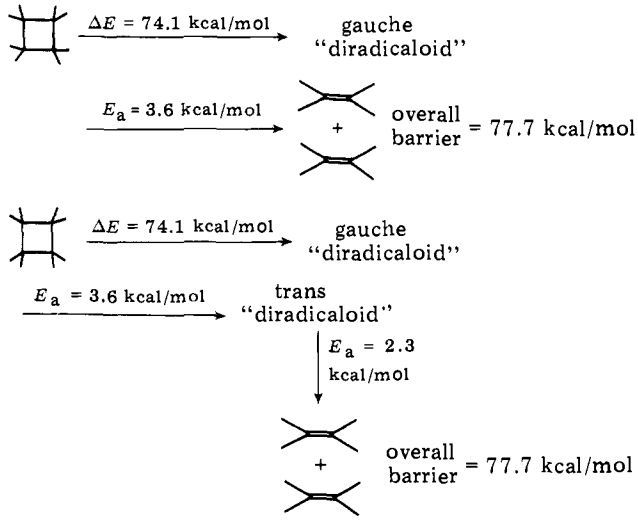

Scheme II

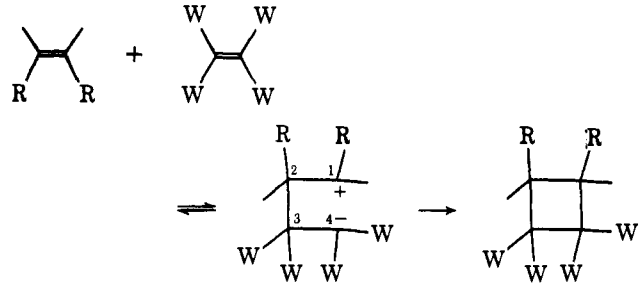

cisoid
biradicaloid (CB)

As we have mentioned in the previous section, as reaction polarity increases, the $[_2\pi_s + _2\pi_s]$ cycloaddition reaction system jumps onto a pericyclic path increasingly earlier along the reaction coordinate. *Thus, a reduction in stereorandomization is expected to accompany an increase in polarity if the operative mechanism is* $[_2\pi_s + _2\pi_s]$. On the other hand, if a TB mechanism is operative, an increase in polarity via substitution should increase the stability and lifetime of the TB diradicaloid. As a result, increased stereorandomization is expected. Finally, no correlation between polarity and stereorandomization due to competing $[_2\pi_s + _2\pi_a]$ paths is clearly discernible.

A systematic study of the polarity-stereoselectivity relationship has not yet been made. However, the available experimental evidence does suggest that in many nonionic cycloadditions $(2\pi + 2\pi)$, an increase in polarity is accompanied by an increase in stereoretention. An example is given below.

		% cis olefin	% trans olefin	$I_D - A_A$,[14] eV	Ref
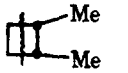		62	38	~10.8	15
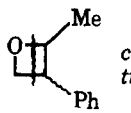	*cis-*	72	28	~8.0	
	trans-	5	95	~8.0	16

In a recent study, Segal[17] investigated by means of ab initio computations the mechanism of the thermal decompositions of cyclobutane to two ethylenes. The results of this study are shown in Scheme I. It is clearly seen that the overall activation energies for a distorted $[_2\pi_s + _2\pi_s]$ mechanism and a TB mechanism are *identical.*

All these results taken together seem to imply that thermal *nonionic* $[2\pi + 2\pi]$ cycloadditions may well occur via a distorted antiaromatic $[_2\pi_s + _2\pi_s]$ path rather than the nonaromatic TB path, in contrast to the currently accepted viewpoint.

(b) The currently accepted mechanism of thermal *ionic* $[2\pi + 2\pi]$ cycloadditions[18-24] is shown in Scheme II. The key feature of this mechanism involves a CB dipolar intermediate devoid of 1-4 bonding. By contrast, we have argued that most ionic $[2\pi + 2\pi]$ cycloadditions are effectively pericyclic $[_2\pi_s + _2\pi_s]$ reactions involving formation of an M intermediate[25] which is pericyclically bonded.

Before turning to the differentiating data, we enumerate four types of mechanistic evidence which can be accounted for by *either mechanism:*

(i) Trapping of intermediate.[20,21]

(ii) Rate response to polar solvents.[19,22]

(iii) The sign and magnitude of $\Delta V^\dagger$ and $\Delta S^\dagger$.[22,23]

(iv) Measurable isomerization of the cycloaddends.[18]

The differentiating pieces of evidence are as follows:

(i) Ionic $[2\pi + 2\pi]$ cycloadditions *are highly stereoselective*

Scheme III

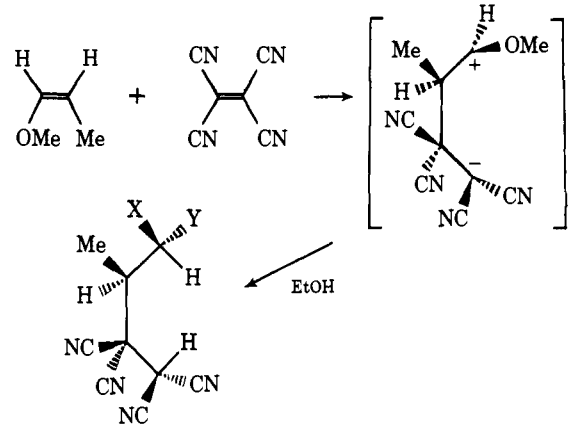

X = OEt; Y = OMe 80%
X = OMe; Y = OEt 4%

or even stereospecific. A tabulation of experimental results can be found in ref 25a. These results are incompatible with the CB mechanism because a "configuration holding" mechanism in the presumably nonpericyclic intermediate is necessary to account for the observed stereoselectivity. This mechanism was proposed to be Coulombic attraction between the ends of the dipole. However, in the point charge approximation, rotation in the intermediate could occur without impairing Coulombic attraction. Furthermore, our recent calculations need to be cited as relevant evidence against the Coulombic argument.[25a] These calculations have shown that a TB approach is favored but most likely needs additional activation energy in order to lead to the cyclobutane adduct. As a result, a $[_2\pi_s + _2\pi_s]$ approach, which is not as favorable as a TB approach but which leads to product without necessitating bond rotation, becomes the preferred path. Furthermore, the $[_2\pi_s + _2\pi_s]$ mechanism accounts for stereoselectivity because the M intermediate has pericyclic character.

M intermediate CB intermediate
(:N = nucleophile)

(ii) Trapping of the intermediate is stereospecific in a manner consistent with the presence of 1-4 bonding.[20] Thus, as illustrated in Scheme III, the intermediate formed by *cis*-propenyl methyl ether and TCNE can be trapped at 0 °C with 95% stereoselectivity.

If the intermediate had no 1-4 pericyclic bonding, the alcohol would add from either of two possible directions. Since addition is only from the outside,[20,21] there must then be some 1-4 bonding.

(c) The stereochemical predictions regarding thermal nonionic $[4\pi + 2\pi]$ cycloadditions are similar to those derived from the Woodward-Hoffmann analysis[1] of pericyclic reactions.

(d) Thermal ionic $[4\pi + 2\pi]$ cycloadditions are predicted to occur via a $[_4\pi_s + _2\pi_s]$ mechanism. The pertinent qualitative PE surface is analogous to that shown in Figure 6b. An N* intermediate is formed and the consequences of such a molecular species on the reaction coordinate can be very interesting. For example, such an intermediate may react chemically with solvent or solute.

The incursion of intermediates in ionic $[4\pi + 2\pi]$ cycloadditions has been recognized in several cases.[22,26] A possible example is given in Scheme IV.[27]

(e) Nonionic $[2\pi + 2\pi]$ photocycloadditions can occur via

Scheme IV

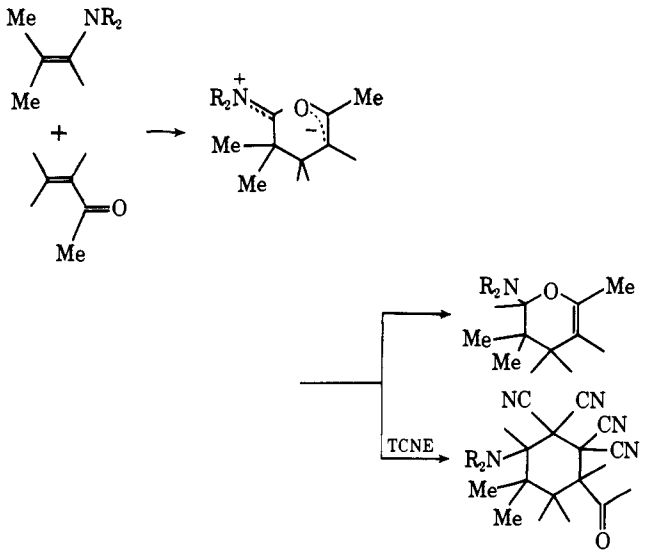

the intermediacy of exciplexes. Recent experimental results have revealed that such molecular species are on the reaction coordinate for $[2\pi + 2\pi]$ photocycloadditions.[28] Ionic $[2\pi + 2\pi]$ photocycloadditions have yet to be studied.

Acknowledgment. This work was supported by a NATO Grant (in collaboration with Professor F. Bernardi) and an A. P. Sloan Fellowship (1976-1978) to N.D.E.

References and Notes

(1) (a) R. B. Woodward and R. Hoffmann, *J. Am. Chem. Soc.*, **87**, 395 (1965); (b) R. Hoffmann and R. B. Woodward, *ibid.*, **87**, 2046 (1965); (c) R. B. Woodward and R. Hoffmann, *ibid.*, **87**, 2511 (1965); (d) "The Conservation of Orbital Symmetry", Verlag Chemie, Weinheim/Bergstr., Germany, 1970; (e) H. C. Longuet-Higgins and E. Abrahamson, *J. Am. Chem. Soc.*, **87**, 2045 (1965).

(2) See part 1: N. D. Epiotis and S. Shaik, *J. Am. Chem. Soc.*, preceding paper in this issue.

(3) For a discussion of symmetry and spin adaptation of wave functions, see S. P. McGlynn, L. G. Vanquickenborne, M. Kinoshita, and D. G. Caroll, "Introduction to Applied Quantum Chemistry", Holt, Rinehart and Winston, New York, N.Y., 1972.

(4) The matrix elements are written in an abbreviated form, e.g., $\langle HO|\hat{H}|LU\rangle \equiv HO\text{–}LU$.

(5) An M intermediate is described by a wave function having a major charge transfer and a minor local excitation contribution.

(6) A $\equiv'^{*}$ intermediate is described by a wave function having an equal no-bond and diexcitation contribution.

(7) A detailed discussion of nonradiative processes can be found in (a) C. Zener, *Proc. R. Soc. London, Ser. A*, **137**, 696 (1932); (b) L. Landau, *Phys. Z. Sowjetunion* **2**, 46 (1932); (c) G. W. Robinson and R. P. Frosch, *J. Chem. Phys.*, **37**, 1962 (1962); (d) *ibid.*, **38**, 1187 (1963); (e) J. Jortner, S. A. Rice, and R. M. Hochstrasser, *Adv. Photochem.*, **7**, 149 (1969); (f) J. Jortner, *Pure Appl. Chem.*, **27**, 389 (1971).

(8) Similar mechanisms of $[{}_2\pi_s + {}_2\pi_s]$ photoreactions have been proposed by (a) J. Michl, *Fortschr. Chem. Forsch.*, **46**, 1 (1974); (b) *Pure Appl. Chem.*, **41**, 507 (1975); (c) W. Th. A. M. Van der Lugt and L. J. Oosterhoff, *J. Am. Chem. Soc.*, **91**, 6042 (1969).

(9) An O intermediate is described by a wave function with a major charge transfer and diexcitation (Ψ_S) contributions.

(10) For related discussion of solvent effect on the shape of PE surfaces, see (a) L. Salem, *J. Am. Chem. Soc.*, **96**, 3486 (1974); (b) W. G. Dauben, L. Salem, and N. J. Turro, *Acc. Chem. Res.*, **8**, 41 (1975); (c) L. Salem, *Science*, **191**, 882 (1976).

(11) An N* intermediate is described by a wave function having a major charge transfer and a minor no-bond contribution.

(12) The N'* intermediate arises from the avoided crossing of DA and D^+A^-.

(13) A configuration which cannot mix with any other constitutes a nonpericyclic state. A state arising from configuration mixing due to bonding interactions along two pairs of uniting atoms constitutes a pericyclic state.

(14) Ionization potential (I) values are taken from D. W. Turner, *Adv. Phys. Org. Chem.*, **4**, 30 (1960). Electron affinity values (A) are taken from P. D. Burrow, J. A. Michejda, and K. D. Jordan, *J. Am. Chem. Soc.*, **98**, 6392 (1976).

(15) H. R. Gerberich and W. D. Walters, *J. Am. Chem. Soc.*, **83**, 3935 (1961).

(16) G. Jones, II, and J. C. Staires, private communication.

(17) G. A. Segal, *J. Am. Chem. Soc.*, **96**, 7892 (1974).

(18) R. Hulsgen and G. Steiner, *J. Am. Chem. Soc.*, **95**, 5054, 5055, 5056 (1973).

(19) R. Huisgen and G. Steiner, *Tetrahedron Lett.*, 3763 (1973).

(20) R. Huisgen, R. Schug, and G. Steiner, *Angew. Chem., Int. Ed. Engl.*, **13**, 80, 81 (1974).

(21) I. Karle, J. Flippen, R. Huisgen, and R. Schug, *J. Am. Chem. Soc.*, **97**, 5285 (1975).

(22) R. Gompper, *Angew. Chem., Int. Ed. Engl.*, **8**, 312 (1969).

(23) W. J. LeNoble and R. Mukhtar, *J. Am. Chem. Soc.*, **97**, 5938 (1975).

(24) (a) L. A. Paquette, M. J. Broadhurst, L. K. Read, and J. Clardy, *J. Am. Chem. Soc.*, **95**, 4639 (1973); (b) S. Proskow, H. E. Simmons, and T. L. Cairns, *ibid.*, **88**, 5254 (1966).

(25) (a) N. D. Epiotis, R. L. Yates, D. Carlberg, and F. Bernardi, *J. Am. Chem. Soc.*, **98**, 453 (1976); (b) N. D. Epiotis and S. Shaik in "Progress in Theoretical Organic Chemistry", Vol. 2, I. G. Csizmadia, Ed., Elsevier, Amsterdam, 1977.

(26) V. D. Kiselev and J. G. Miller, *J. Am. Chem. Soc.*, **97**, 4036 (1975).

(27) I. F. Fleming and M. H. Krager, *J. Chem. Soc. C*, 226 (1967).

(28) For example, see F. D. Lewis and C. E. Hoyle, *J. Am. Chem. Soc.*, **99**, 3779 (1977).